Stress and Phase Purity Analyses of Diamond Films Deposited through Laser-Assisted Combustion Synthesis

ARTICLE *in* ACS APPLIED MATERIALS & INTERFACES · SEPTEMBER 2011

Impact Factor: 6.72 · DOI: 10.1021/am201010h · Source: PubMed

ACS APPLIED MATERIALS & INTERFACES

RESEARCH ARTICLE

www.acsami.org

Stress and Phase Purity Analyses of Diamond Films Deposited through Laser-Assisted Combustion Synthesis

T. Guillemet,[†,§] Z. Q. Xie,[†] Y. S. Zhou,[†] J. B. Park,[†] A. Veillere,[†,§] W. Xiong,[†] J. M. Heintz,[§] J. F. Silvain,[§] N. Chandra,[‡] and Y. F. Lu*[,†]

[†]Department of Electrical Engineering and [‡]Department of Mechanical and Materials Engineering, University of Nebraska—Lincoln, Lincoln, Nebraska 68588-0511, United States

[§]Université Bordeaux 1, Institut de Chimie de la Matière Condensée de Bordeaux (ICMCB), CNRS, 33608 Pessac, France

ABSTRACT: Diamond films were deposited on silicon and tungsten carbide substrates in open air through laser-assisted combustion synthesis. Laser-induced resonant excitation of ethylene molecules was achieved in the combustion process to promote diamond growth rate. In addition to microstructure study by scanning electron microscopy, Raman spectroscopy was used to analyze the phase purity and residual stress of the diamond films. High-purity diamond films were obtained through laser-assisted combustion synthesis. The levels of residual stress were in agreement with corresponding thermal expansion coefficients of diamond, silicon, and tungsten carbide. Diamond-film purity increases while residual stress decreases with an increasing film thickness. Diamond films deposited on silicon substrates exhibit higher purity and lower residual stress than those deposited on tungsten carbide substrates.

KEYWORDS: diamond films, laser-assisted combustion synthesis, laser-induced resonant excitation, Raman spectroscopy, residual stress

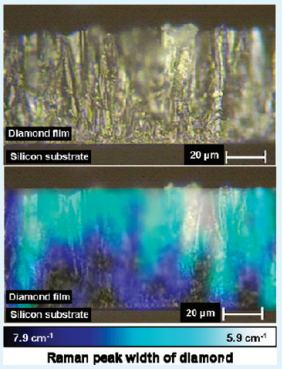

1. INTRODUCTION

Diamond is of significant importance because of its wide range of superlative properties including extreme hardness, high thermal conductivity, high electrical resistivity, low friction coefficient, and high chemical inertness. Because of its outstanding properties, diamond has been intensively investigated for decades.[1] Additionally, replacing former high-pressure-high-temperature methods, various chemical vapor deposition (CVD) techniques including hot filament CVD,[2] microwave plasma CVD,[3] and combustion CVD[4−7] now enable the synthesis of diamond with high flexibility and low capital costs, and stimulate a wide spectrum of diamond applications, such as heat-spreaders[8,9] and superhard coatings.[10] Since its discovery by Hirose and Kondo in 1988,[7] combustion-flame CVD has demonstrated numerous advantages over conventional CVD methods, such as open-air synthesis, flexibility, scalable nature, low-cost, and high growth rate.[1,4−7]

Although other studies have been previously carried out on laser-assisted combustion synthesis of diamond films in open air,[11−14] clear understanding and quantification of both diamond phase purity and internal residual stresses in diamond films deposited through this technique are still lacking. Phase purity and residual stress are two key parameters in integrating diamond films with nondiamond substrates and major limiting factors in diamond film applications. Low diamond purity due to defects, impurities, and nondiamond carbon contents drastically affects diamond properties, such as hardness and thermal conductivity. Residual stress leads to cracks, poor adhesion, and even delamination, thus strongly degrades the mechanical reliability of diamond films. Residual stress in a diamond film consists of two major parts. One is the thermal stress, caused by the mismatch of thermal expansion coefficients (CTEs) between diamond and the substrate material, which develops during cooling from deposition temperature. The other is the intrinsic stress (also called growth stress) that is the cumulative result of grain boundary formation and impurities incorporation into the film during deposition.[15−18] Diamond films generally exhibit a lower CTE compared with conventional substrate materials. Therefore, thermal stress in diamond films is often compressive. On the other hand, the intrinsic stress is often revealed to be tensile. To integrate the as-deposited diamond films into devices, clear understanding about their crystal quality and stress level is required.

Raman spectroscopy is a fast, nondestructive, and widely employed method to characterize diamond films and evaluate their phase purity and residual stress. Diamond has a highly recognizable signature in Raman scattering with a sharp peak at 1332 cm^{-1}.[19] The full width at half-maximum (fwhm) of the diamond line is representative of the diamond phase purity, whereas its shift can be related to the level of residual stress in the film. A compressive or tensile stress induces a shift in the diamond peak to higher or lower wavenumbers, respectively.[15,17] Representatives of nondiamond carbon features, such as D-band (disordered graphite, at 1375 cm^{-1}), G-band (ordered graphite, at 1580 cm^{-1}), and the broad band of amorphous carbon (around 1500 cm^{-1}), also provide information about the nondiamond carbons existing in the film.[19,20]

Received: July 31, 2011
Accepted: September 26, 2011
Published: September 26, 2011

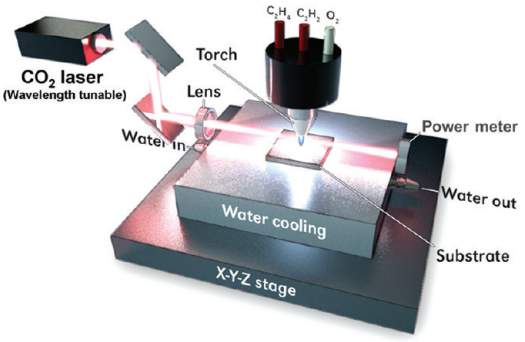

Figure 1. Laser-assisted combustion CVD setup for diamond film deposition.

We investigated in this study the deposition of diamond films on silicon (Si) and cemented tungsten carbide (WC-Co) substrates through laser-assisted combustion CVD in open air. A multienergy deposition method was deployed by coupling the thermal energy from a combustion flame with the energy of a high-power wavelength tunable CO_2 laser. The laser wavelength was tuned to 10.532 μm in order to match a vibrational mode of ethylene molecules, thus achieving the laser-resonant excitation of one type of carbon precursors. Figure 1 shows a schematic of the experimental setup. It was reported that the laser-induced vibrational excitation of precursor molecules increased the concentration of active species in the flame and was beneficial to the diamond growth, both from texture and growth rate aspects.[11−14] Scanning electron microscopic (SEM) micrograph was used to investigate the cross-sectional and top-surface morphology of the diamond films. Raman spectroscopic investigations were carried out to evaluate film quality and level of residual stress. According to the SEM analysis, it was confirmed that the laser-assisted combustion CVD process enabled fast deposition of thick diamond films onto the silicon and WC-Co substrates. Raman spectroscopy showed that high-phase purity diamond films were deposited. The residual stress investigation provided results in good agreement with expectations, because the residual stresses measured were consistent with the respective CTEs of diamond, silicon, and WC-Co. The evolution of diamond phase purity and residual stress with film thickness were discussed. It was found that the substrate material had strong influence on both phase purity and residual stress of the diamond films.

2. EXPERIMENTAL DETAILS

2.1. Diamond Films Deposition. The diamond deposition setup used in this study was similar to that reported in our previous studies,[11−14] as shown in Figure 1, consisting of a wavelength tunable CO_2 laser (XL1000, PRC Laser Corporation) associated to a combustion system. A combustion torch with a diameter of 1.5 mm was used. A gas mixture containing acetylene (C_2H_2, 99.999%), ethylene (C_2H_4, 99.6%) and oxygen (O_2, 99.996%) was used as gas precursors with a volume ratio of 1:1:2, respectively. The laser beam was guided through the combustion flame using a ZnSe convex lens with a focal distance of 25.6 cm. The distance between the lens and the nozzle was 30 cm. The distance between the flame inner cone and the top of the substrate was maintained around 0.8 mm. The laser was operated in a continuous wave mode. Its output power was 800 W and its wavelength was set to 10.532 μm in order to match the CH_2 vibrational mode of ethylene molecules (wagging mode),[14] thus achieving the resonant excitation of the ethylene molecules. The substrate temperature was monitored using an infrared pyrometer (OS3752, Omega Engineering, Inc.) and regulated using a water-cooling stage. The stage was attached to an X-Y-Z translation system to position the substrate toward the torch. The substrate temperature was maintained around 780 °C during diamond deposition.

2.2. Substrates. Diamond films were deposited on commercial Si(100) and cemented WC substrates (BS-6S, 6 wt % Co, Basic Carbide Corp.). Silicon and WC-Co substrates were chosen because they were frequently used materials in electrical and mechanical engineering respectively, one being the most important material for contemporary semiconductor industry, the other being a typical hard material used for cutting tools. The dimensions of silicon and WC-Co substrates were $10 \times 10 \times 0.6$ and $12.7 \times 12.7 \times 1.6$ mm^3, respectively. The substrates were ultrasonically cleaned for 20 min in acetone prior to diamond deposition. No seeding was needed for diamond growth on WC-Co substrates. However, silicon substrates were seeded using ultrafine diamond powder (average diameter of 250 nm) through ultrasonic treatment in a mixture of diamond/ethanol solution, with 0.1 g of diamond powder dispersed in 10 mL of ethanol, to enhance the nucleation of diamond crystals on the Si(100) surfaces.

2.3. Microstructural Analyses. The microstructure of the deposited diamond films were investigated using a SEM (XL-30, Philips Electronics). Film thicknesses were measured using a stylus profiler (XP-2, Ambios Technology). Raman spectroscopic investigations were performed using a micro-Raman spectrometer (inVia H 18415, Renishaw) with a 514.5 nm argon ion laser as the excitation source. A point-focus mode was used during the diamond peak width evaluation. A line-focus mode was used during the diamond peak shift evaluations in order to decrease the bulk power density in the sample and avoid unwanted tensile-like peak shift due to local heating.[21] The laser power was 50 mW. The point-shaped spot was about 1 μm in diameter. The line-shaped spot showed dimensions of about 40 μm in length and 1 μm in width. The grating used was 3000 lines/mm in order to achieve the highest resolution. By coupling with a 1014 pixels CCD camera, a resolution of 0.31 cm^{-1}/pixel was obtained. However, Raman spectroscopy is a localized measurement collecting information only from the laser spot covered regions. To get more accurate values of peak widths and peak shifts, we used a mapping technique to scan a large area of the sample. Each mapping was about 5000 μm^2 in area, including about 250 individual scans. These scans provide an average value for the as-mapped parameter (either diamond peak width or diamond peak shift), and thus more representative values for the diamond films studied. The diamond peak position was determined automatically using the curve-fitting option integrated in the operation software. All Raman spectra were taken at the center of the deposited diamond films.

3. RESULTS AND DISCUSSIONS

3.1. Microstructure of the Diamond Films. SEM micrographs of diamond films deposited on the WC-Co and Si substrates under the same conditions are shown in images a and b in Figure 2, respectively. Diamond films were deposited on the substrates as circular spots of about 1 cm in diameter for 1 h deposition. SEM micrographs showed that the laser-assisted deposition process enabled fast deposition of thick diamond films on both types of substrates. The films obtained are dense and homogeneous polycrystalline diamond films, consisting of randomly oriented diamond crystals. In Figure 2a, spherical grains were observed on top of the diamond film deposited on a WC-Co substrate. The spherical grains were ascribed to the formation of cobalt particles that diffused from the coating-substrate interface to the film top surface.[22,23] Larger diamond grains are observed on WC-Co than those on Si for the same

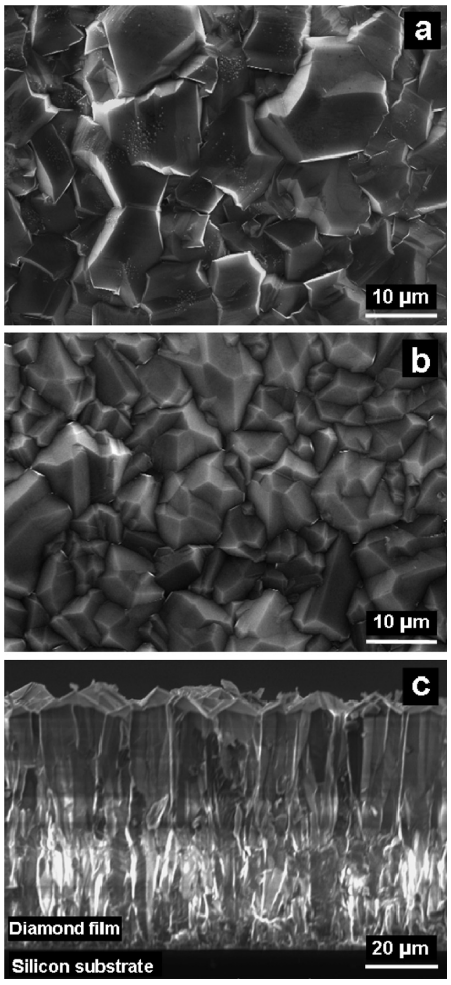

Figure 2. SEM micrographs of diamond films deposited through laser-assisted combustion CVD: (a) top surface, t = 60 min on WC-Co, (b) top surface, t = 60 min on Si, (c) cross-section, t = 120 min on Si.

deposition time. This was ascribed to the fact that diamond nucleation was promoted on WC-Co by the carbon content embedded in the substrate and its initial roughness, thus no need for additional seeding.[23] The growth rates are about 31 μm/h on silicon and 50 μm/h on WC-Co, which are much higher than those of conventional CVD techniques.[1−3] This is of significant importance since low growth rate in diamond CVD techniques is one of the critical limiting factors for diamond films applications. According to the cross-sectional SEM micrograph of a diamond film deposited on silicon shown in Figure 2c, the diamond growth occurred following the formation of characteristic columnar structures, with diamond grains size increasing with film thickness. The diamond−silicon interface exhibited good integrity, without obvious voids or holes in the film or around the substrate interface.

3.2. Raman Spectroscopic Investigations. Panels a and b in Figure 3 show Raman spectra obtained from the diamond films of various thicknesses deposited on Si and WC-Co, respectively. All of the films exhibited sharp diamond peaks located around 1332 cm^{-1}. D-band (1375 cm^{-1}) and amorphous carbon broad band (1500 cm^{-1}) were also observed showing much lower intensities. Moreover, to consider the respective scattering efficiency of diamond, graphite, and amorphous carbon (1, 50, and

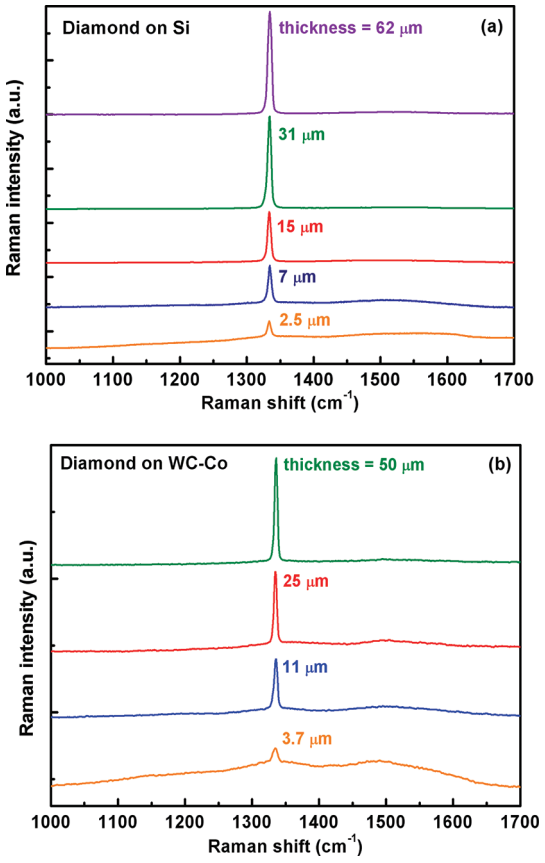

Figure 3. Raman spectra of diamond films of various thicknesses deposited on (a) Si and (b) WC-Co substrates.

233, respectively),[24] growth of high-phase purity diamond films could be concluded. Intensities of the diamond peak and amorphous carbon broad-band increased and decreased, respectively, with an increasing film thickness on both types of substrates, suggesting a phase purity enhancement with increasing film thickness. The Raman spectra also show that the substrate material exhibited obvious influence on the growth of the diamond films. More nondiamond carbon species were observed on the diamond films deposited on the WC-Co substrates compared to those deposited on silicon. This is ascribed to the carbide and cobalt content embedded into WC-Co substrates, which may diffuse into the films during deposition.[23]

3.2.1. Diamond Quality Analysis. Widths of diamond Raman peak are plotted as a function of film thickness in Figure 4a. It confirms quantitatively that the laser-assisted deposition process enables deposition of high-phase purity diamond films. Average diamond peak widths obtained from Raman mappings were located between 5.6 and 8.1 cm^{-1} on Si and 7.2 and 9.0 cm^{-1} on WC-Co, with minimum peak widths of 4 and 6 cm^{-1} on Si and WC-Co, respectively, which was close to that of high-quality type IIa diamond (3.1 cm^{-1}).[1] The error bars represent the total distribution of values recorded from the mapping. The plotted points represent the centers of the distributions. The diamond phase purity was also quantified through the calculation of the diamond quality parameter[2]

$$Q_{[514\text{nm}]} = \frac{I_{\text{Diamond}}}{\left([(I)]_{\text{Diamond}} + \frac{I_{\text{a-carbon}}}{233}\right)} 100\ (\%) \qquad (1)$$

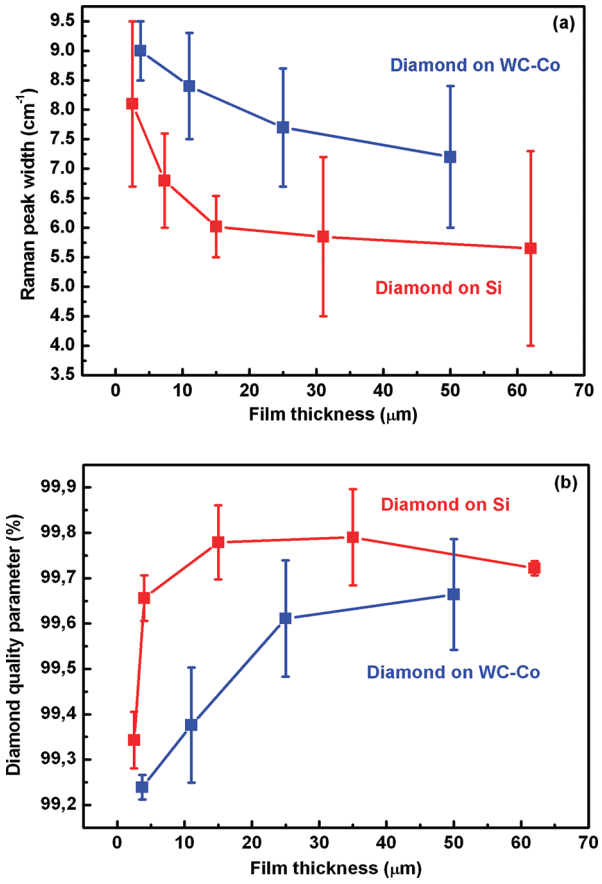

Figure 4. (a) Raman peak width and (b) diamond quality parameters of diamond films deposited on Si and WC-Co as a function of film thickness.

where $I_{Diamond}$ is the intensity of the diamond line, and $I_{a\text{-}Carbon}$, is the sum of the intensities of the observed nondiamond carbon features. As shown in Figure 4b, the values of diamond quality parameter are located between 99.2 and 99.8%, indicating high-phase-purity diamond films. This was ascribed to the laser-resonant excitation process, in which efficient laser energy coupling stimulated the decomposition of the precursors and significantly increased concentration of atomic hydrogen and OH radicals. The increased atomic hydrogen and OH radical concentrations generated an etching environment for removing nondiamond carbon species.[1,6] The laser-induced vibrational excitation of ethylene molecules thus improves the purity of the deposited diamond films.

Figure 4 confirms quantitatively that the diamond phase purity is proportional to the film thickness. Indeed, diamond peak width and quality parameter decreases and increases respectively when the film get thicker, suggesting that the sp^3 carbon content increases with respect to film thickness. This phenomenon was ascribed to the larger diamond grains by increasing film thickness, which reduced grain boundaries irradiated by the laser in Raman spectroscopy. Since impurities tend to locate at the grain boundaries, the overall film quality was improved if the number of grain boundaries decreased. Figure 4 also confirms that the substrate material has a strong influence on the quality of the diamond films. Diamond films deposited on the WC-Co substrates exhibited larger diamond peak widths and lower quality parameter. This again was ascribed to the diffusion of nondiamond particles, such as cobalt and carbides, into the film during the deposition process on the WC-Co substrates. Diamond film phase purity is enhanced on silicon by the use of diamond powder as seeding layer prior to the deposition.

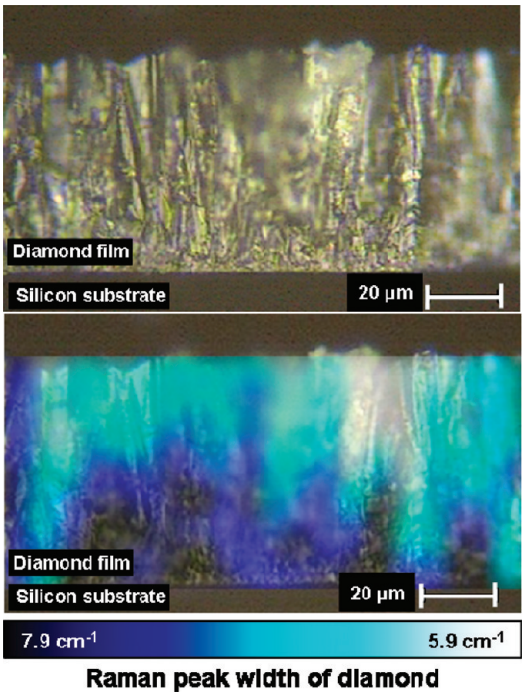

Figure 5. Cross-sectional optical image and Raman mapping of a diamond film deposited on Si; parameter recorded: Raman peak width of diamond.

Figure 5 shows a colored cross-sectional Raman mapping of a diamond film deposited on a silicon substrate, which confirms the proportional diamond quality improvement with film thickness increase. It was observed that the width of the diamond peak decreased from the diamond−substrate interface to the top surface of the diamond film as the diamond grain size increases.

3.2.2. Residual Stress Analysis. In this study, Raman spectroscopy was also used to measure the level of residual stress existing in the diamond films. Diamond films deposited on both types of substrates exhibited peak shifts to higher wave numbers compared to stress-free diamond at 1332 cm^{-1}, revealing that the residual stress in the diamond films was compressive on both types of substrates. For diamond films deposited on both substrates under similar conditions, larger diamond peak shifts were observed on the diamond films deposited on WC-Co than that deposited on Si, with typical shifts at 1337 cm^{-1} on WC-Co and 1333 cm^{-1} on Si. These results are consistent with individual CTEs of diamond, silicon and WC-Co (at 293 K: $\alpha_{Diamond}$ = 1.0 × 10^{-6} $°C^{-1}$, α_{Si} = 2.59 × 10^{-6} $°C^{-1}$, $\alpha_{WC\text{-}Co}$ = 4.42 × 10^{-6} $°C^{-1}$). Because diamond has a lower CTE than Si and WC-Co, a compressive thermal stress is expected. Also, the higher amplitude of residual stress in diamond films deposited on WC-Co compared to those deposited on Si is consistent with the higher CTE mismatch between diamond and WC-Co compared to that between diamond and Si.

The degrees of shift and splitting of the diamond Raman line are proportional to the level of biaxial residual stress inside the diamond films. Ager and Drory developed a general model relating singlet and doublet phonon scattering to the internal stress.[25] We used this model to calculate the level of residual

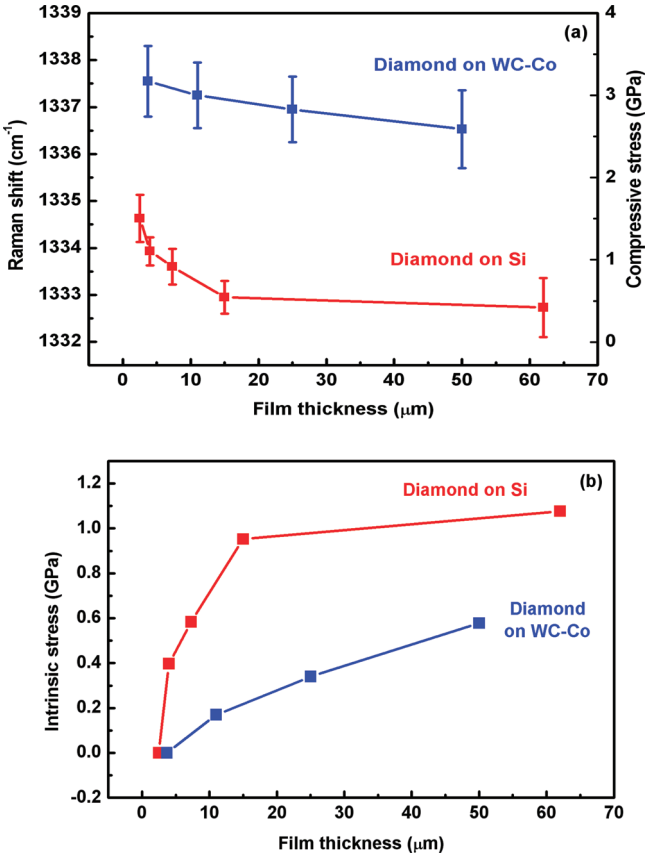

Figure 6. (a) Raman peak shift and corresponding compressive stress in diamond films deposited on Si and WC-Co as a function of film thickness; (b) intrinsic stress in diamond films deposited on Si and WC-Co substrates as a function of film thickness.

stress in the deposited diamond films through the following relationship

$$\sigma = -0.567 \times (\nu_m - \nu_o)\ (\text{GPa}) \quad (2)$$

where ν_m is the observed peak position and ν_o is the Raman peak shift for an unstressed diamond film (1332 cm^{-1}).

The thermal stress induced by the thermal expansion mismatch between the diamond film and the substrate can be calculated using the following equation[10]

$$\sigma_{\text{thermal}} = \left(\frac{E_{\text{Diamond}}}{1-\nu_{\text{Diamond}}}\right) \times \int_{T_0}^{T} (\alpha_{\text{Film}} - \alpha_{\text{substrate}})\mathrm{d}T\ (\text{GPa}) \quad (3)$$

where E_{Diamond} is the Young's modulus of diamond (E_{Diamond} = 1150 GPa), ν_{Diamond} is the Poisson's ratio of diamond (ν_{Diamond} = 0.07), α_{Film} and $\alpha_{\text{Substrate}}$ are the thermal expansion coefficients of the diamond film and the substrate material, respectively, and T and T_0 are the deposition and room temperatures, respectively ($\Delta T = T - T_0$ = 760 K). A positive or negative sign stands for a tensile or compressive thermal stress, respectively. To take into account the variation of CTE with temperature, the following equation was used for each material: $\alpha = (\alpha_{T_o} + \alpha_T)/2$, α_{T_o} being the CTE at room temperature (293 K), α_T being the CTE at deposition temperature (at 1053 K: $\alpha_{\text{Diamond}} = 4.58 \times 10^{-6}\ ^\circ\text{C}^{-1}$, $\alpha_{\text{Si}} = 4.45 \times 10^{-6}\ ^\circ\text{C}^{-1}$, $\alpha_{\text{WC-Co}} = 6.50 \times 10^{-6}\ ^\circ\text{C}^{-1}$). Although it is a thin-film approximation, eq 5 provides an estimation of the thermal stress induced by the CTE mismatch.

The corresponding calculated thermal stresses are −0.70 and −2.52 GPa in diamond films deposited on silicon and WC-Co, respectively. The measured residual stresses at low film thickness (2.5 μm on Si and 3.7 μm on WC-Co) are respectively −1.49 and −3.14 GPa on Si and WC-Co substrates, respectively. The respective signs and amplitude of thermal stresses calculated are consistent with the residual stresses measured by Raman spectroscopy. The gap between the theoretical values and the measured values is ascribed to the domain size effect observed in Raman spectroscopy.[26]

Figure 6a represents the diamond peak shift measured in the diamond films of various thicknesses deposited on the silicon and WC-Co substrates. The corresponding compressive stress calculated using eq 1 is shown on a parallel scale. The total residual stress decreased with increasing film thickness on both silicon and WC-Co substrates. This was ascribed to an increase in intrinsic stress due to the formation of grain boundaries and growth strains during the diamond deposition process, thus decreasing the total residual stress. It confirms that the intrinsic stress is a tensile stress. Assuming that the intrinsic stress is close to zero for thinner films, the intrinsic stress in diamond films was plotted. Figure 6b shows the increase of intrinsic stress with increasing film thickness. Maximum intrinsic stresses of 1.1 and 0.6 GPa in diamond films deposited on Si and WC-Co were calculated, respectively. Although intrinsic stress is lower in diamond films deposited on WC-Co substrates than on silicon substrates, the diamond films were observed to delaminate much more easily from WC-Co substrates during the experiments. It is believed that the high thermal expansion mismatch and the diffusion of nondiamond particles into the film strongly affect the adhesion strength between the film and the substrate, thus being responsible for the peeling-off of the diamond films from WC-Co substrates. In addition, the residual stress in thick diamond films deposited on silicon is close to zero, which could be responsible for the good adhesion of the diamond films to silicon substrates.

4. CONCLUSIONS

High-phase purity diamond films were deposited on silicon and WC-Co substrates in open air using laser-assisted combustion synthesis. High growth rates were achieved (31 μm/h on silicon, and 50 μm/h on WC-Co). SEM micrographs showed that the diamond films exhibited polycrystalline structure consisting of faceted and randomly oriented diamond crystals. Raman spectroscopic investigations revealed that the laser-resonant excitation of ethylene precursor molecules enabled an efficient energy coupling between the flame and the laser, leading to the fast deposition of diamond films with high phase purity. Diamond phase purity was found to increase with increasing film thickness, which was related to the enlargement of diamond grain size with increasing film thickness. Residual stress was found to be compressive in diamond films deposited on both types of substrates and decreases with increasing film thickness, due to the increase of the intrinsic stress. Diamond films deposited on WC-Co substrates exhibited lower phase purity and higher residual stress due to the diffusion of nondiamond particles into the films (especially cobalt particles) and large CTE mismatch with diamond. Diamond films integrate better with silicon than with WC-Co substrates.

AUTHOR INFORMATION

Corresponding Author
*Tel: 1-402-472-8323. Fax: 1-402-472-4732. E-mail: ylu2@unl.edu.

ACKNOWLEDGMENT

The authors thank Dr. D. R. Alexander in the Department of Electrical Engineering at the University of Nebraska−Lincoln for providing convenient access to the SEM. This work was financially supported by the U.S. Office of Naval Research (ONR) through the Multidisciplinary University Research Initiative (MURI N00014-05-1-0432) program and Grant N00014-09-1-0943. We are grateful to Dr. I. Perez from ONR for his advice and support.

REFERENCES

(1) Asmussen, J.; Reinhard, D. K. In *Diamond Films Handbook*; Marcel Dekker: New York, 2002.
(2) Back, G. W.; Fabisiak, K.; Klimek, L.; Kozanecki, M.; Staryga, E. *Opt. Mater.* **2008**, *30*, 770–773.
(3) Jiang, X.; Klages, C. P. *Diamond Relat. Mater.* **1993**, *2*, 1112–1113.
(4) Hirose, Y.; Amanuma, S. *J. Appl. Phys.* **1990**, *68* (12), 6401–6405.
(5) Kim, J. S.; Cappelli, M. A. *J. Appl. Phys.* **1992**, *72* (11), 5461–5466.
(6) Donnet, J. B.; Oulanti, H.; Le Huu, T.; Schmitt, M. *Carbon* **2006**, *44*, 374–380.
(7) Hirose, H.; Koaki, K. EP 324538, 1988.
(8) Fiegl, B.; Kunhert, R.; Schwarzbauer, H.; Koch, F. *Diamond Relat. Mater.* **1994**, *3*, 658–662.
(9) Glaser, A.; Jentsch, H. G.; Rosiwal, S. M.; Ludtke, A.; Singer, R. F. *Mater. Sci. Eng., B* **2006**, *127*, 186–192.
(10) Xu, Z. Q.; Lev, L.; Lukitsch, M.; Kumar, A. *J. Mater. Res.* **2007**, *22* (4), 1012–1017.
(11) Ling, H.; Sun, J.; Han, Y. X.; Gebre, T.; Xie, Z. Q.; Zhao, M.; Lu, Y. F. *J. Appl. Phys.* **2009**, *105*, 014901.
(12) Ling, H.; Xie, Z. Q.; Gao, Y.; Gebre, T.; Shen, X. K.; Lu, Y. F. *J. Appl. Phys.* **2009**, *105*, 064901.
(13) Xie, Z. Q.; Zhou, Y. S.; He, X. N.; Gao, Y.; Park, J. B.; Ling, H.; Jiang, L.; Lu, Y. F. *Cryst. Growth Des.* **2010**, *10* (4), 1762–1766.
(14) Xie, Z. Q.; He, X. N.; Hu, W.; Guillemet, T.; Park, J. B.; Zhou, Y. S.; Bail, J.; Gao, Y.; Zeng, X. C.; Jiang, L.; Lu, Y. F. *Cryst. Growth Des.* **2010**, *10* (11), 4928–4933.
(15) Nakamura, Y.; Sakagami, S.; Amamoto, Y.; Watanabe, Y. *Thin Solid Films* **1997**, *308−309*, 249–253.
(16) Fan, Q. H.; Fernandes, A.; Pereira, E.; Gracio, J. *Diamond Relat. Mater.* **1999**, *8*, 645–650.
(17) Fan, Q. H.; Gracio, J.; Pereira, E. *Diamond Relat. Mater.* **2000**, *9*, 1739–1743.
(18) Kim, J. G.; Yu, J. *Mater. Sci. Eng., B* **1998**, *57*, 24–27.
(19) Knight, D. S.; White, W. B. *J. Mater. Res.* **1989**, *4* (2), 385–393.
(20) Kromka, A.; Breza, J.; Kadlecikova, M.; Janik, J.; Balon, F. *Carbon* **2005**, *43*, 425–429.
(21) Kouteva-Arguirova, S.; Seifert, W.; Kittler, M.; Reif, J. *Mater. Sci. Eng., B* **2003**, *102*, 37–42.
(22) Donnet, J. B.; Paulmier, D.; Oulanti, H.; Le Huu, T. *Carbon* **2004**, *42*, 2215–2221.
(23) Veillère, A.; Guillemet, T.; Xie, Z. Q.; Zuhlke, C. A.; Alexander, D. R.; Silvain, J. F.; Heintz, J. M.; Chandra, N.; Lu, Y. F. *Appl. Mater. Interfaces* **2011**, *3*, 1134–1139.
(24) Leeds, S. M.; Davis, T. J.; May, P. W.; Pickard, C. D. O.; Ashfold, M. N. R. *Diamond Relat. Mater.* **1998**, *7*, 233–237.
(25) Ager, J. W.; Drory, M. D. *Phys. Rev. B* **1993**, *48* (4), 2601–2607.
(26) Nemanich, R. J.; Bergman, L.; LeGrice, Y. M.; Turner, K. F.; Humphreys, T. P. *Proc. SPIE* **1991**, *2*, 1437.